

Surface Wave Tomography of the Arctic from Rayleigh and Love Wave Group Velocity Dispersion Data

A. I. Seredkina^{a, b, *}

^a*Institute of the Earth's Crust, Siberian Branch, Russian Academy of Sciences, Irkutsk, 664033 Russia*

^b*Institute of Terrestrial Magnetism, Ionosphere and Radio Wave Propagation, Russian Academy of Sciences, Troitsk, Moscow, 108840 Russia*

**e-mail: ale@crust.irk.ru*

Received December 11, 2017; revised December 21, 2017; accepted May 28, 2018

Abstract—The results of studying the deep structure of the Earth's crust and upper mantle of the Arctic from surface wave data are presented. For this purpose, based on the frequency-time analysis procedure, a representative dataset of group velocity dispersion curves of Rayleigh and Love waves (1555 and 1265 paths, respectively) in the period range from 10 to 250 s is obtained. With the use of a two-dimensional tomography technique for a spherical surface, group velocity distributions are calculated at separate periods. Overall, 18 maps for each type of surface waves are constructed and the horizontal resolution of the mapping is estimated. For four tectonically different regions of the Arctic, the dispersion curves calculated from the tomography results are inverted to the velocity sections of *SV*- and *SH*-waves. Based on the obtained distributions, the main large-scale features are analyzed in the deep structure of the Earth's crust and upper mantle of the Arctic, and the revealed velocity irregularities are correlated to various geological structures. The results of the study are of considerable interest for further constructing the three-dimensional model of the shear wave velocity distribution and for studying the anisotropic properties of the upper mantle of the Arctic, as well as for building the geodynamical models of the region.

Keywords: surface wave tomography, group velocities, Rayleigh and Love waves, upper mantle, Arctic

DOI: 10.1134/S106935131903008X

INTRODUCTION

The Arctic region comprises geologically and tectonically different structures (Fig. 1). Its continental part is composed of the ancient platforms and shields, as well as the younger fold belts of Eurasia and North America (Zonenshain and Natapov, 1987; Zonenshain et al., 1990). The oceanic part of the study area includes the shelves of the marginal seas, deep-water ocean basins with their separating Lomonosov, Alpha-Mendelev Ridges and the Gakkel spreading Ridge with ultra-slow spreading velocities varying from 0.6 cm/yr in the east to 1.3 cm/yr in the west (DeMets et al., 1994).

Currently, the active development and production of minerals, including hydrocarbons of the Russian shelf, is taking place in the Arctic. Progress in economic activities, in turn, requires detailed estimates of the seismic hazard of the territory. A more accurate seismic hazard assessment and elucidation of many disputable issues of modern tectonics and geodynamics are greatly promoted by the new data about the deep structure of the region of interest.

The lack of seismic stations and nonuniform distribution of earthquake epicenters in the high northern latitudes impose significant limitations on the studies

of the deep structure of the Earth's crust and upper mantle of the Arctic. A review of the existing deep structure models is presented in (Gaina et al., 2014). We note that the main currently known information about the region under study is contained in the global models (Bijwaard et al., 1998; Shapiro and Ritzwoller, 2002; Zhou et al., 2006; Ekström, 2011, Laske et al., 2013; Schaeffer and Lebedev, 2013; etc.). However, these models have a rather low resolution for the Arctic compared to the other regions of the world. Similar problems of resolution also exist in the rather scarce regional studies (Levshin et al., 2001; Yakovlev et al., 2012), whereas the results of more detailed works based on the data of body waves (Allen et al., 2002; Darbyshire, 2003; Kumar et al., 2005; Lebedeva-Ivanova et al., 2006; Jokat and Schmidt-Aursch, 2007; etc.) and surface waves (Bruneton et al., 2004; Darbyshire et al., 2004; Pilidou et al., 2004; 2005; Levshin et al., 2007; Chen et al., 2007; Pedersen et al., 2013) are very local. Thus, the purpose of this work is to study the deep structure of the Arctic by the method of surface wave tomography by constructing the maps of Rayleigh and Love wave group velocity distributions in the period range from 10 to 250 s and subsequent interpretation of these maps.

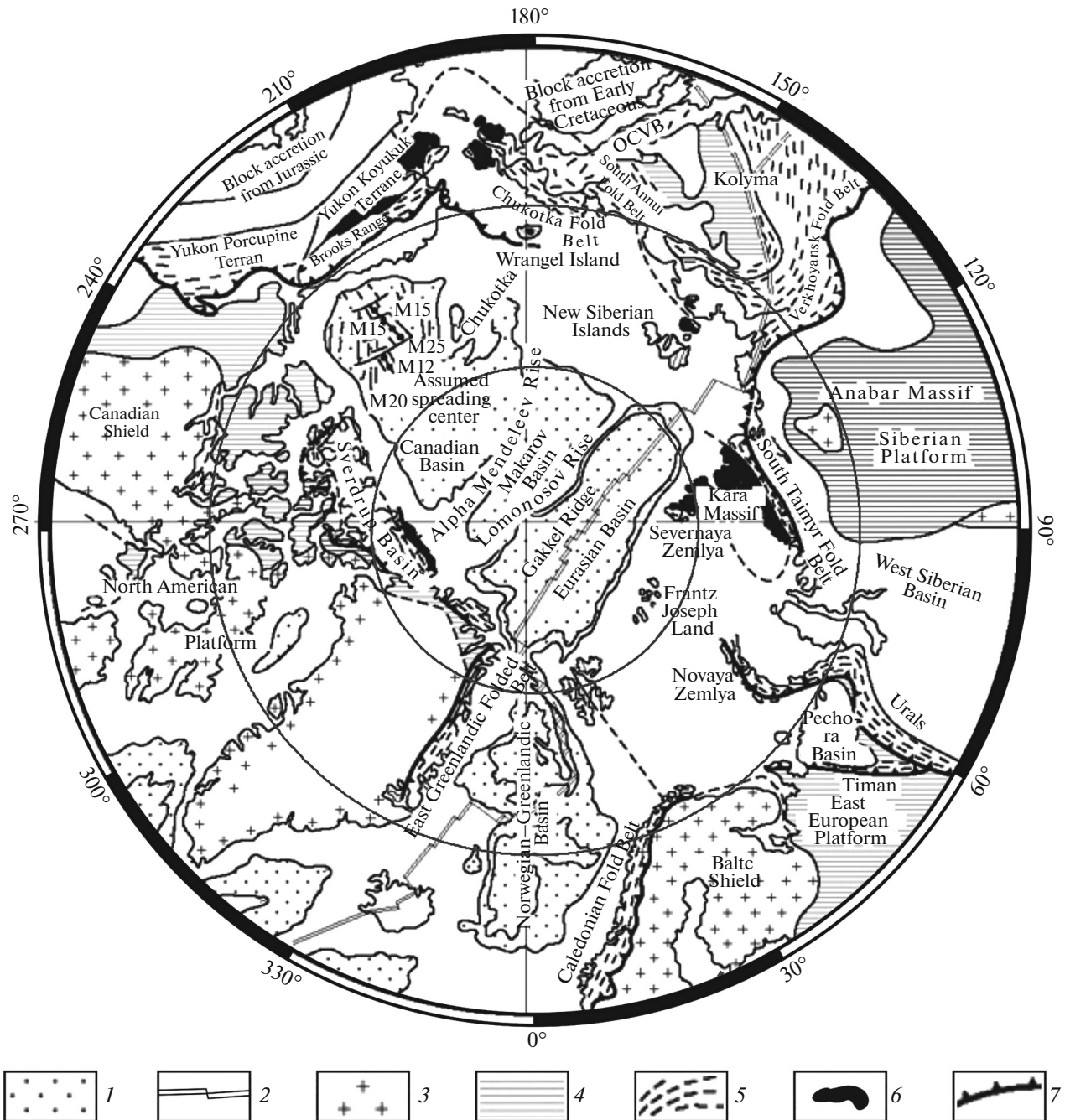


Fig. 1. Main geological structures of the Arctic according to (Zonenshyn and Natapov, 1987). 1, ocean basins deeper than 2000 m, 2000 and 3000 m isobaths are shown; 2, active spreading center; 3–5, continental structures (3, shields; 4, platforms; 5, orogenic belts); 6, ancient massifs, remains of the Arctida continent; 7, folding front; M12, M15, M20, M25, Mesozoic magnetic anomalies.

INITIAL DATA AND STUDY METHODS

This study is based on the records of surface waves from the remote earthquakes at the LHZ and LHT channels of digital broadband seismic stations of the IRIS, GEOSCOPE, GEOFON networks, as well as the GLISN virtual network which was relatively recently installed in Greenland (Fig. 2a). Overall, 38 earthquakes with $M_w \geq 5.1$ that occurred in 1996 to 2015 in

Iceland, close to Greenland, in Alaska and northeastern Eurasia, along the Gakkel Ridge and the Aleutian Arc were analyzed (Fig. 2a). The group velocity dispersion curves were calculated along the epicenter–station paths. The distances from the epicenters of the earthquakes selected for the analysis to the recording stations ranged from 2000 to 10000 km. In most cases, this allowed us to identify the fundamental mode of surface waves within the period range from 10 to 250 s

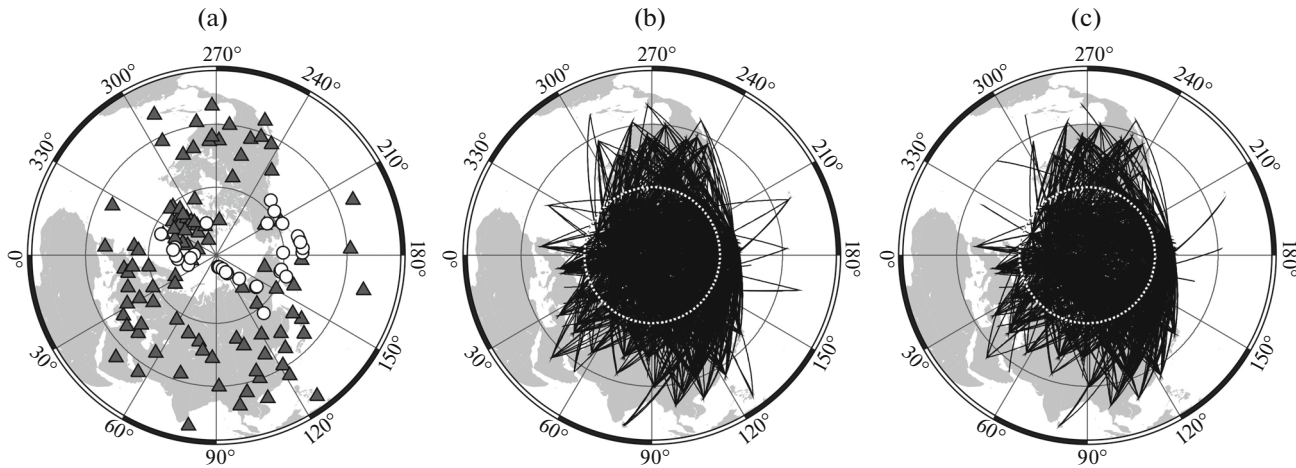


Fig. 2. (a) Positions of earthquake epicenters (circles) and seismic stations (triangles) selected for analysis; obtained seismic paths for (b) Rayleigh and (c) Love waves.

which, according to (Ritzwoller and Levshin, 1998; Yanovskaya, 2015) corresponds to a depth of about 500 km.

The group velocity dispersion curves of the fundamental mode of surface waves were calculated with the use of the frequency–time analysis (FTAN, or the Russian acronym SVAN) procedure (Levshin et al., 1986). Only the records with a high signal-to-noise ratio were used in the analysis. Figure 3 shows an example of processing for the earthquake with $M_w = 6.3$ that occurred on March 6, 2005 on the Gakkel Ridge and was recorded by the Ala-Archa (AAK) station. Using this procedure, we obtained totally 1555 dispersion curves for Rayleigh waves (Fig. 2b) and 1265 curves for Love waves (Fig. 2c).

The determination errors of group velocities were estimated from the reproducibility of the dispersion curves: the curves with close paths were averaged, and root mean square (rms) deviations of the velocities from their average values at individual periods were calculated. The average dispersion curves for the study region for Rayleigh and Love waves with their errors are shown in Fig. 4. From this figure it can be seen that the minimal rms deviations are confined to the interval $T = 25–150$ s, whereas the rms deviations at the other periods are somewhat higher. The wide scatter of group velocity values at short periods ($T < 25$ s) is probably associated with not only the calculation errors but also with strong heterogeneity of the Earth's crust, especially in its upper part. We also note the worse reproducibility of the dispersion curves for Love waves. In general, the obtained results agree with the previous data (Ritzwoller and Levshin, 1998).

The maps of group velocity distribution were calculated by the two-dimensional tomography method for a spherical surface (Yanovskaya et al., 2000; Yanovskaya, 2001; 2015). For each map, we estimated its resolution by calculating the effective averaging

radius (R) (Yanovskaya, 2001; 2015; Yanovskaya and Kozhevnikov, 2003) which mainly depends on the density of coverage of a particular segment of the studied region by seismic paths. The previously calculated synthetic tests have shown (Yanovskaya, 2015) that the values of the radius of the equivalent smoothing area fairly well agree with the results of the checkerboard test. In our case, the highest resolution (400–600 km for Rayleigh waves and 500–700 km for Love waves) is observed in the central part of the study area (north of 70° N) and in northeast Eurasia and Alaska (Fig. 5). At the periphery, particularly in southern Greenland and Canada, the effective averaging radius is larger. Besides, the horizontal resolution deteriorates in a regular manner with the increase of the period because fewer seismic paths are used for the analysis. As a limiting value of an acceptable resolution, we assumed $R = 1000$ km, similar to (Yanovskaya and Kozhevnikov, 2003).

The analysis of the group velocity distribution maps for the individual periods provides an overall idea of the large-scale horizontal inhomogeneities in the upper mantle of the Arctic region. For qualitatively assessing the depth of the revealed velocity anomalies for four tectonically different regions, the local dispersion curves of Rayleigh and Love waves obtained from the results of the tomography were inverted to the velocity sections of the S -waves.

The parameters of the model media satisfying the local dispersion curves were calculated by minimizing the residuals between the observed and calculated group velocity values by the conjugate gradient method (Yanovskaya, 2015). As a starting model, we used a medium with two plane-parallel crustal layers and eleven mantle layers in which the velocity linearly varies with depth on the half-space. The S -wave velocities in the crustal and mantle layers and the thicknesses of the crustal layers were used as the varied parameters. The EUNaseis (Artemieva and Thybo,

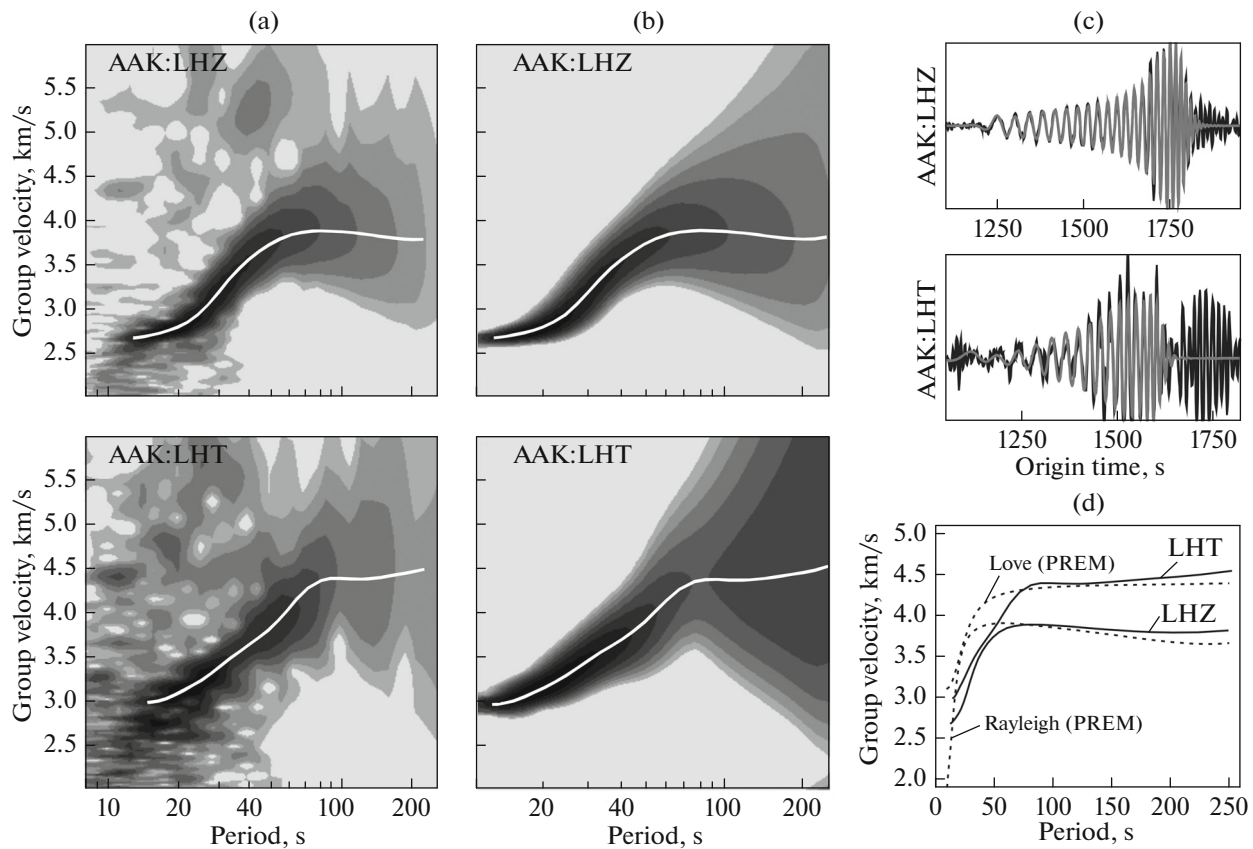


Fig. 3. Example of processing the earthquake of March 6, 2005 ($M_w = 6.3$) recorded at vertical (LHZ) and transverse (LHT) components of the AAK station ($\Delta = 4775$ km): FTAN (SVAN) diagrams of (a) initial and (b) filtered signals (group velocity dispersion curve is shown by white line); (c) seismograms before (black lines) and after (gray lines) filtering; (d) obtained group velocity dispersion curves in comparison with dispersion curves calculated for the PREM model (Dziewonski and Anderson, 1981).

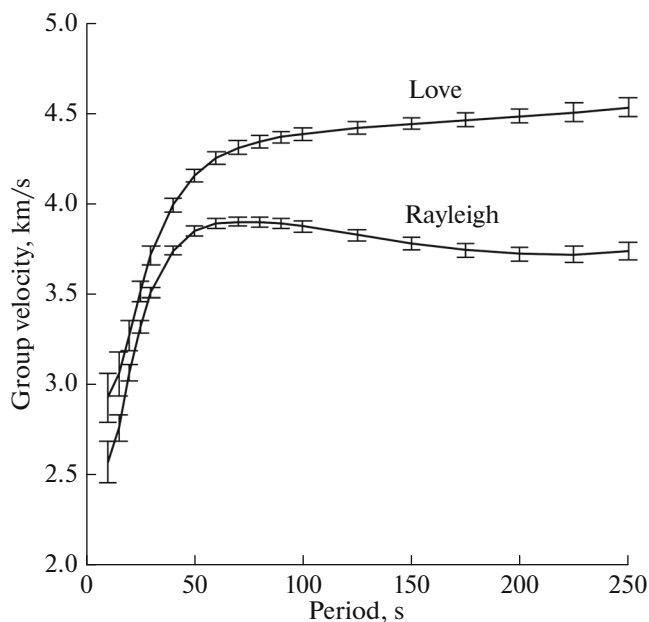


Fig. 4. Region-average dispersion curves of Rayleigh and Love waves with error estimates of group velocity determinations.

2013) and CRUST 1.0 models (Laske et al., 2013) were assumed as the starting models for the crust, and the spherically symmetric PREM model (Dziewonski and Anderson, 1981) was used for the mantle. Initially, based on the group velocities of Rayleigh waves, the velocity sections of the SV -waves were calculated. Then these sections were used as the starting models for constructing the velocity sections of the SH -waves satisfying the dispersion curves of Love waves. For testing the stability of the obtained results, we constructed a section averaged over these two solutions, and repeated the calculations again for both types of surface waves based on this average section. In all cases, the velocity sections obtained in this way practically coincided with the results of the initial calculations.

RESULTS AND DISCUSSION

In accordance with the assumed procedure, the distributions of group velocities were calculated separately for each oscillation period. For the period intervals 10–30, 30–100, and 100–250 s, the period step was 5, 10, and 25 s, respectively. Thus, 18 maps were

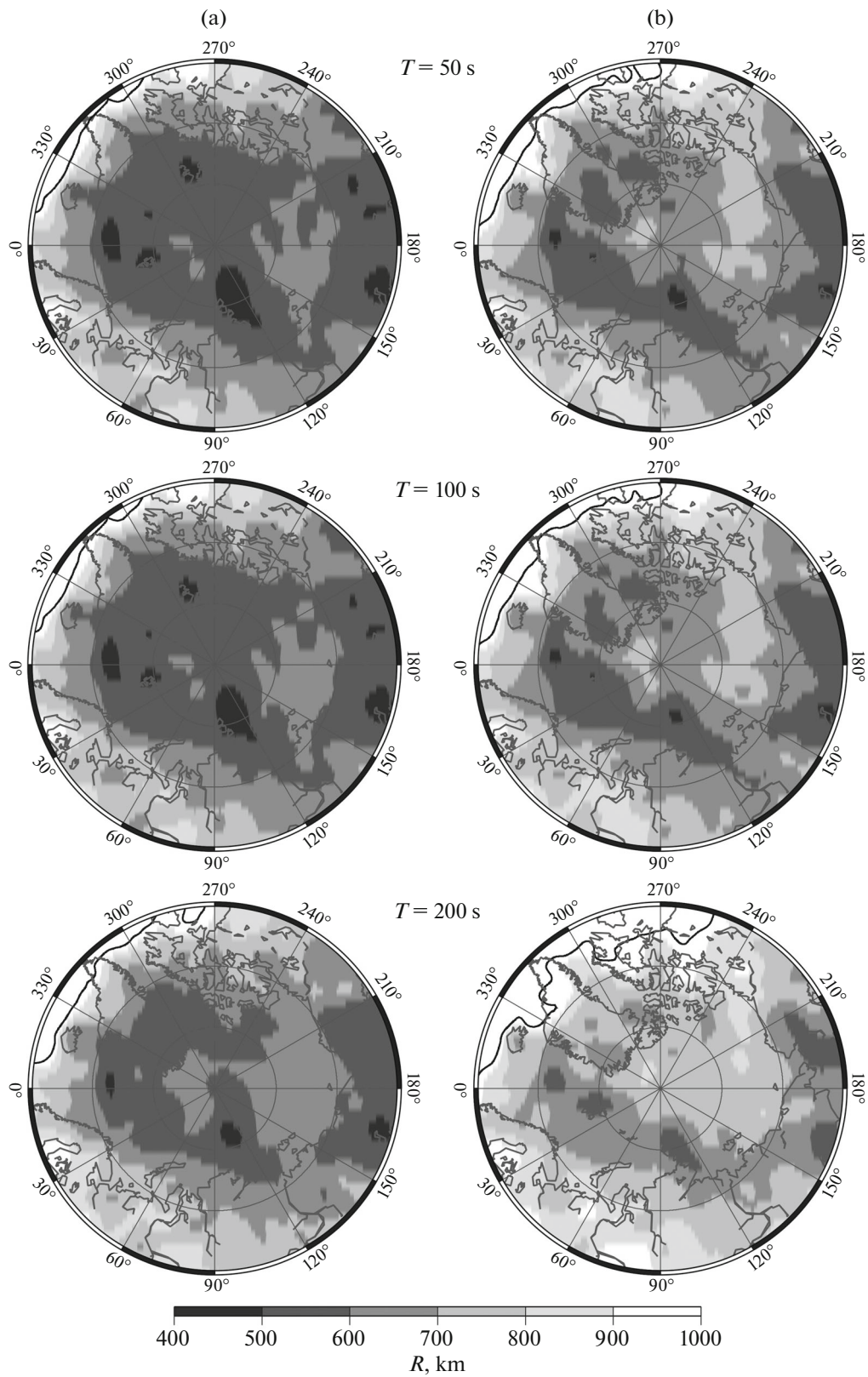


Fig. 5. Examples of maps of effective averaging radius (R , km) for (a) Rayleigh and (b) Love waves for oscillation periods of 50, 100, and 200 s. Boundary $R = 1000$ km is shown by black line.

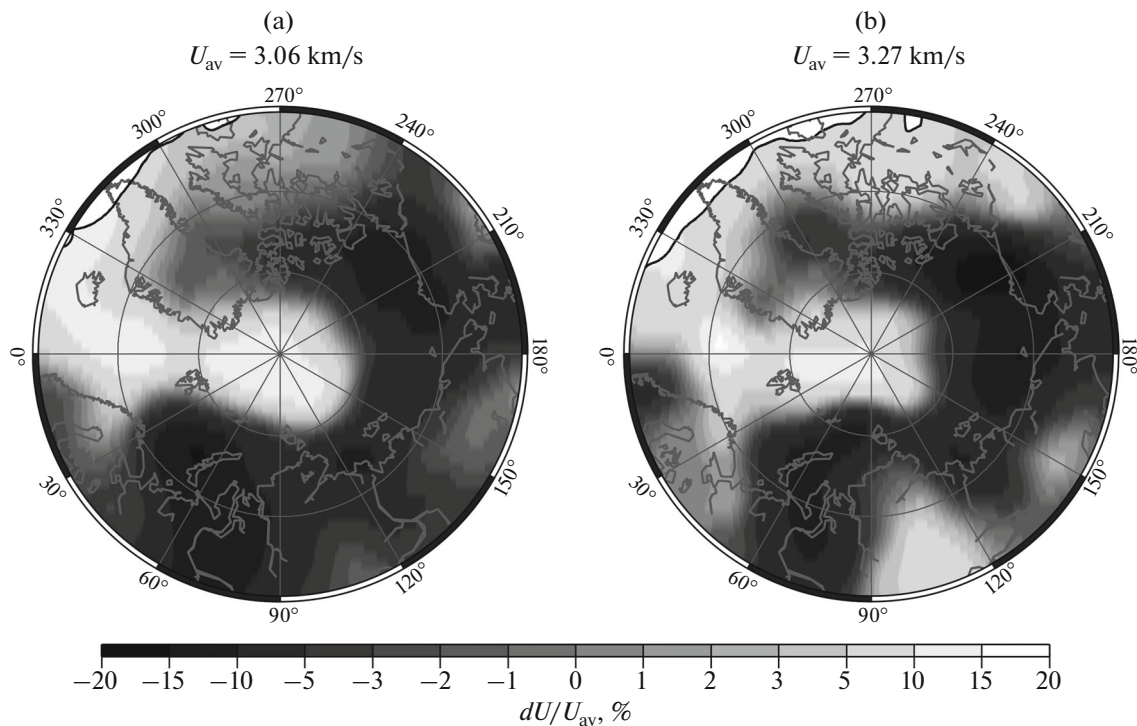


Fig. 6. Group velocity variations of (a) Rayleigh and (b) Love waves relative to average values (U_{av}) for oscillation period 20 s.

constructed for each type of surface waves. In the interpretation of the obtained maps and comparison of group velocity variations with the geological structure of the studied region (Fig. 1) it should be remembered that Rayleigh and Love waves have different sensitivity to the parameters of the medium and different penetration depth (Yanovskaya, 2015).

For both types of surface waves, the maps for the period of 20 s (Fig. 6) reflect the structural traits of the Earth's crust, whereas the group velocities widely vary from -20 to $+20\%$. The minima of group velocities in these maps are confined to the basins of marginal seas and to the large sedimentary basins in the north of Eurasia: the Yenisei–Khatanga and Lena–Anabar basins (Drachev, 2016). Moreover, the intensity of the revealed minima is correlated to the thickness of the sediments (Gramberg et al., 1999). The basins of the Arctic Ocean and the Greenland and Norwegian deep seas are marked with high surface wave velocities, which is probably due to the crustal thinning beneath these regions (Laske et al., 2013; Artemieva and Thybo, 2013). The pattern of the dispersion for the oscillation period of 50 s (Figs. 7, 8) for the continental part of the study region is determined by both the influence of the crust and the upper part of the mantle, and, to a certain extent, reflects the variations in crustal thickness beneath different regions.

The maps for longer periods (up to 150 s) reflect the distribution of the horizontal inhomogeneities in the mantle part of the lithosphere and in the astheno-

sphere, whereas the character of the dispersion of the surface wave velocities at the periods larger than 150 s is affected by the subasthenospheric mantle layers. The maximum values of the variations of the group velocities (up to $+5\%$) at these periods are confined to the Canadian and Baltic shields, which indicates the large thickness of the lithosphere (up to 280 km) and high shear wave velocities in it (Chen et al., 2007; Olson et al., 2007; Darbyshire et al., 2013; Grad et al., 2014). High velocities ($+1$ to $+3\%$) are also characteristic of the East European and Siberian platforms; moreover, with the growth of the period, this peculiarity beneath the Siberian platform becomes more pronounced. The minimum velocities (up to -10%) are associated with the fold belts of northeastern Eurasia and Alaska, as well as with the Bering Sea Basin where the recent subduction of the Pacific Plate is taking place.

The revealed trends are clearly expressed in the velocity sections of the S -waves calculated for four tectonically different structures of the studied region: the Amundsen ocean Basin, the Baltic Shield, the Barents Sea shelf, and the Verkhoyansk–Kolyma fold belt (Fig. 9). At the periods up to 60 s for Rayleigh waves and up to 80 s for Love waves, the highest group velocities are observed in the deep-water Amundsen basin (Fig. 9a), which has a thinned oceanic crust (Laske et al., 2013; Gaina et al., 2014). This crustal thinning is also reflected in the maximal velocities of the S -waves down to the depth of about 50 km relative to the other

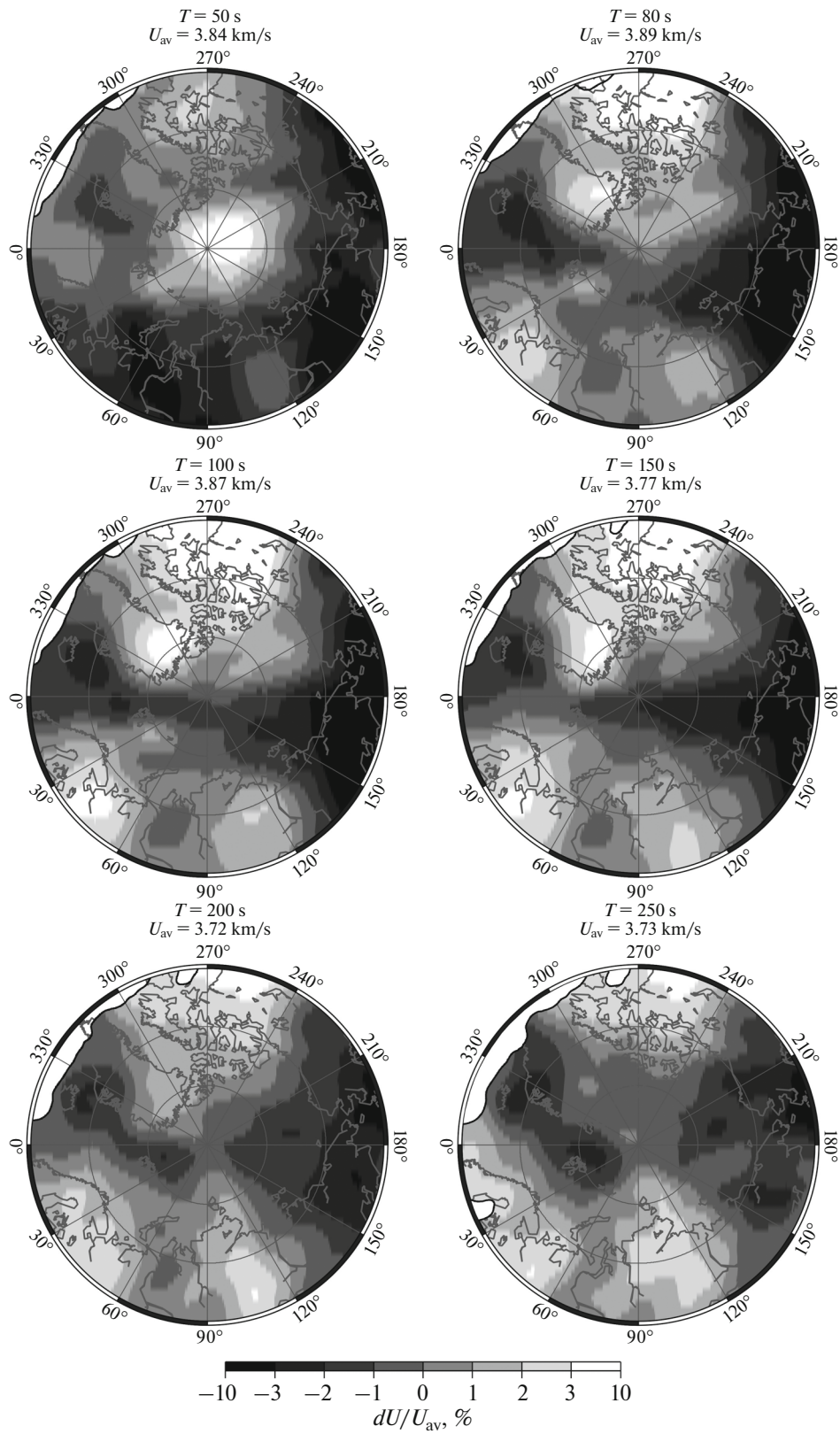


Fig. 7. Group velocity variations of Rayleigh waves relative to average values (U_{av}) for oscillation periods 50, 80, 100, 150, 200, and 250 s.

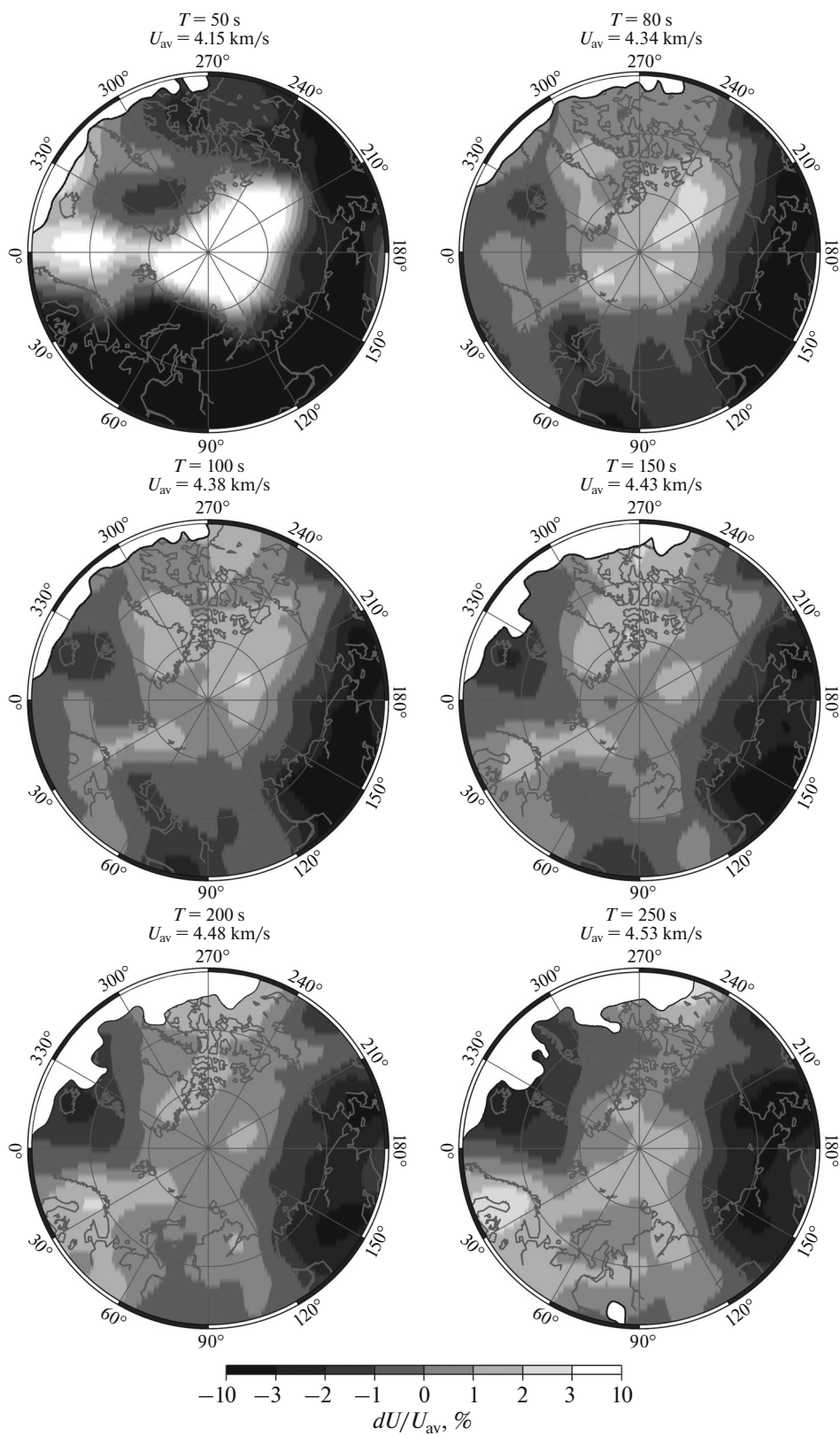


Fig. 8. Group velocity variations of Love waves relative to average values (U_{av}) for oscillation periods 50, 80, 100, 150, 200, and 250 s.

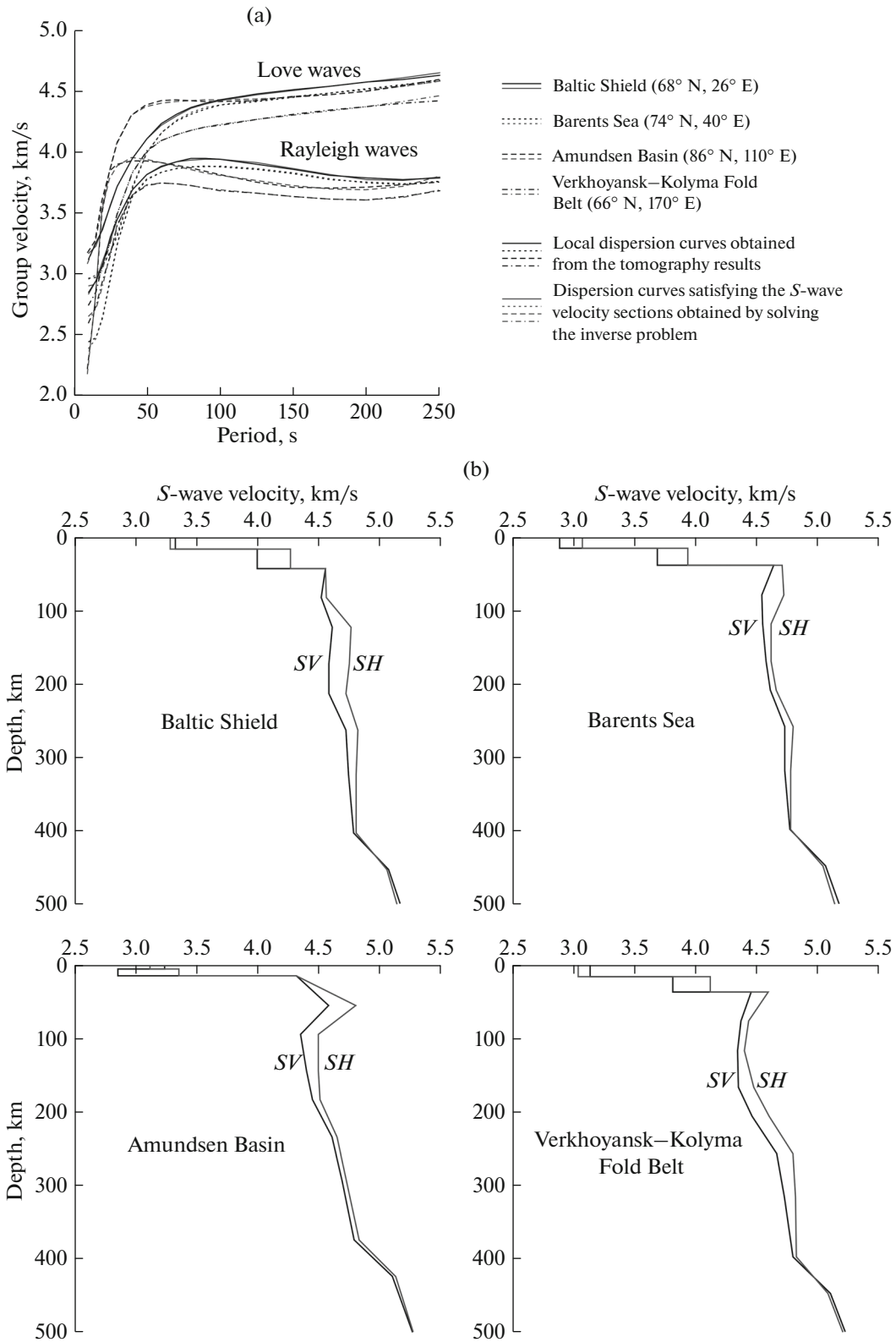


Fig. 9. (a) Dispersion curves of Rayleigh and Love waves and (b) respective velocity sections of *SV*- and *SH*-waves for four tectonically different regions of the Arctic.

considered regions (Fig. 9b). As expected, with the increase of the period, the maximal values of both the group velocities and shear wave velocities are traced beneath the stable Precambrian Baltic Shield. It is worth noting that the obtained velocity section of *SV*-waves closely agrees with the results calculated from the Rayleigh wave phase velocity dispersion data at the LAPNET seismic array (Pedersen et al., 2013). For example, in both models, the *SV*-wave velocities in the depth interval from 50 to 250 km are 4.5–4.6 km/s with the maximum at the depth of about 150 km and a slight decrease in the interval from 160 to 220 km (Fig. 9b). The relatively high shear wave velocities (above 4.5 km/s) are observed in the upper mantle of the Barents Sea. In the previous studies of this region from the group and phase velocities of surface waves (Levshin et al., 2007), where as an example of the inversion, the authors considered the point with the same coordinates (74° N, 40° E), the pattern of the velocity section of *SH*-waves (the maximum at 60–80 km and a smooth decrease of the velocities to 200 km), as well as the absolute values of the group velocities of Rayleigh and Love waves, practically coincide with the results of this work. Certain inconsistency of the *SV*-wave velocity sections in the depth interval from 50 to 100 km is most likely due to the different resolution of the initial data. The minimal values of the *S*-wave velocities for the considered structures are characteristic of the upper mantle of the Verkhoyansk–Kolyma fold belt, which also manifests itself by the dispersion of group velocities of surface waves (Figs. 7, 8, 9a) and is consistent with the results of the previous studies based on the surface waves (Levshin et al., 2001), body waves (Yakovlev et al., 2012), and their joint inversion (Schaeffer and Lebedev, 2013).

In the periods from 50 to 250 s, the maps for the both types of surface waves have a local minimum of the velocities (–3%) in the region of Iceland, most likely associated with the Iceland mantle plume whose depth is estimated from 200 (Pilidou et al., 2004; 2005) to 400 (Bijwaard et al., 1998) and even down to 700 km (Yakovlev et al., 2012). This anomaly is traced hundreds of kilometers north of Iceland, which is consistent with the results of the previous studies (Levshin et al., 2001; Pilidou et al., 2004; 2005) and it can also indicate the presence of a plume beneath the Jan Mayen Island. This plume is identified both based on the geological data (Schilling et al., 1999) and based on the results of regional tomography with a higher horizontal resolution (Rickers et al., 2013).

On the maps of Rayleigh waves (Fig. 7), the Gakkel Ridge at the periods up to 200 s can be traced in the form of the minimum of the group velocities. Remarkably, at the transition from the Eurasian Basin to the continental margin of the Laptev Sea, the rather narrow spreading zone widens and turns into a system of rift troughs, which is reflected by the change of the pattern of seismicity (Avetisov, 1999; Imaeva et al., 2017) and in different geophysical fields (Verhoeve et al., 1996; Kenyon et al., 2008; Andersen et al., 2010),

including the expansion of the zone of low group velocities on the shelf, obtained in this work. Another interesting feature is that with the increase of the period (above 200 s), the maps of Love waves (Fig. 8) have high values of group velocities beneath the Gakkel Ridge, indicating the presence of a significant radial anisotropy at large depths in the mantle, which is apparently characteristic of the centers of slow spreading (Zhou et al., 2006).

It is worth noting that with the growth of the period, velocity variations become smoother, which indicates that at the depths below 400 km the mantle becomes less differentiated in terms of velocities.

CONCLUSIONS

Based on the conducted study, we can conclude that the obtained maps of the distributions of the Rayleigh and Love wave group velocities reflect the structural features of the crust and upper mantle of the Arctic, whereas the detected horizontal velocity irregularities agree with the geological structure of the studied region. The obtained maps are of considerable interest for the subsequent construction of a three-dimensional model of the shear wave velocity distribution and for studying the anisotropic properties of the upper mantle.

ACKNOWLEDGMENTS

I thank Prof. T.B. Yanovskaya (St. Petersburg State University) for providing the software, and Prof. A.L. Levshin (University of Colorado, Boulder, United States) and Dr. V.M. Kozhevnikov, (Institute of the Earth's Crust, Siberian Branch, Russian Academy of Sciences) for their valuable advice and attention to the work.

FUNDING

This work was supported by the Russian Science Foundation, project no. 17-77-10037.

REFERENCES

- Allen, R.M., Nolet, G., Morgan, W.J., Vogfjörð, K., Nettles, M., Ekström, G., Bergsson, B.H., Erlendsson, P., Foulger, G.G., Jakobsdóttir, S., Julian, B.R., Pritchard, M., Ragnarsson, S., and Stefánsson, R., Plume-driven plumbing and crustal formation in Iceland, *J. Geophys. Res.*, 2002, vol. 107, no. B8, 2163. doi 10.1029/2001JB000584
- Andersen, O.B., Knudsen, P., and Berry, P., The DNSC08GRA global marine gravity field from double retracked satellite altimetry, *J. Geod.*, 2010, vol. 84, no. 3, pp. 191–199. doi 10.1007/s00190-009-0355-9
- Artemieva, I.M. and Thybo, H., EUNaseis: a seismic model for Moho and crustal structure in Europe, Greenland, and the North Atlantic region, *Tectonophysics*, 2013, vol. 609, pp. 97–153. <http://dx.doi.org/10.1016/j.tecto.2013.08.004>

- Avetisov, G.P., Geodynamics of the zone of continental continuation of Mid-Arctic earthquakes belt (Laptev Sea), *Phys. Earth Planet. Inter.*, 1999, vol. 114, pp. 59–70.
- Bijwaard, H., Spakman, W., and Engdahl, E.R., Closing the gap between regional and global travel time tomography, *J. Geophys. Res.*, 1998, vol. 103, no. B12, pp. 30055–30078.
- Bruneton, M., Pedersen, H.A., Farra, V., Arndt, N.T., Vacher, P., et al., Complex lithospheric structure under the central Baltic Shield from surface wave tomography, *J. Geophys. Res.*, 2004, vol. 109, B10303. doi 10.1029/2003JB002947
- Chen, C.-W., Rondenay, S., Weeraratne, D.S., and Snyder, D.B., New constraints on the upper mantle structure of the Slave craton from Rayleigh wave inversion, *Geophys. Res. Lett.*, 2007, vol. 34, L10301. doi 10.1029/2007GL029535
- Darbyshire, F.A., Crustal structure across the Canadian High Arctic region from teleseismic receiver function analysis, *Geophys. J. Int.*, 2003, vol. 152, pp. 273–391.
- Darbyshire, F.A., Larsen, T.B., Mosegaard, K., Dahl-Jensen, T., Gudmundsson, O., Bah, T., Gregersen, S., Pedersen, H.A., and Hanka, W., A first detailed look at the Greenland lithosphere and upper mantle using Rayleigh wave tomography, *Geophys. J. Int.*, 2004, vol. 158, pp. 267–286. doi 10.1111/j.1365-246X.2004.02316.x
- Darbyshire, F.A., Eaton, D.W., and Bastow, I.D., Seismic imaging of the lithosphere beneath Hudson Bay: episodic growth of the Laurentian mantle keel, *Earth Planet. Sci. Lett.*, 2013, vol. 373, pp. 179–193. <https://doi.org/10.1016/j.epsl.2013.05.002>
- DeMets, C., Gordon, R.G., Argus, D.F., and Stein, S., Effect of recent revisions to the geomagnetic reversal time scale on estimates of current plate motions, *Geophys. Res. Lett.*, 1994, vol. 21, pp. 2191–2194.
- Drachev, S.S., Fold belts and sedimentary basins of the Eurasian Arctic, *Arktos*, 2016, vol. 2, article no. 21. doi 10.1007/s41063-015-0014-8
- Dziewonski, A.M. and Anderson, D.L., Preliminary Reference Earth Model, *Phys. Earth Planet. Inter.*, 1981, vol. 25, pp. 297–356.
- Eksröm, G., A global model of Love and Rayleigh surface wave dispersion and anisotropy, 25–250 s, *Geophys. J. Int.*, 2011, vol. 187, pp. 1668–1686. doi 10.1111/j.1365-246X.2011.05225.x
- Gaina, C., Medvedev, S., Torsvik, T.H., Koulakov, I., and Werner, S.C., 4D Arctic: a glimpse into the structure and evolution of the Arctic in the light of new geophysical maps, plate tectonics and tomographic models, *Surv. Geophys.*, 2014, vol. 35, pp. 1095–1122. doi 10.1007/s10712-013-9254-y
- Grad, M., Tiira, T., Olsson, S., and Komminaho, K., Seismic lithosphere–asthenosphere boundary beneath the Baltic Shield, *GFF*, 2014, vol. 136, no. 1, pp. 581–598. <https://doi.org/10.1080/11035897.2014.959042>
- Gramberg, I.S., Verba, V.V., Verba, M.L., and Kos'ko M.K., Sedimentary cover thickness map—sedimentary basins in the Arctic, *Polarforschung*, 1999, vol. 69, pp. 243–249.
- Imaeva, L.P. and Kolodez'nikov, I.I., Eds., *Seismotektonika severo-vostochnogo sektora Rossiiskoi Arktiki* (Seismotectonics of the Northeastern Sector of the Russian Arctic), Novosibirsk: SO RAN, 2017.
- Jakovlev, A.V., Bushenkova, N.A., Koulakov, I.Yu., and Dobretsov, N.L., Structure of the upper mantle in the Circum-Arctic region from regional seismic tomography, *Russ. Geol. Geophys.*, 2012, vol. 53, no. 10, pp. 963–971.
- Jokat, W. and Schmidt-Aursch, M.C., Geophysical characteristics of the ultraslow spreading Gakkel Ridge, Arctic Ocean, *Geophys. J. Int.*, 2007, vol. 168, pp. 983–998. doi 10.1111/j.1365-246X.2006.03278.x
- Kenyon, S., Forsberg, R., and Coakley, B., New gravity field for the Arctic, *Eos Trans. AGU*, 2008, vol. 89, no. 32, pp. 289–290. doi 10.1029/2008EO320002
- Kumar, P., Kind, R., Hanka, W., Wylegalla, K., Reigber, Ch., Yuan, X., Woelber, I., Schwintzer, P., Fleming, K., Dahl-Jensen, T., Larsen, T.B., Schweitzer, J., Priestley, K., Gudmundsson, O., and Wolf, D., The lithosphere–asthenosphere boundary in the North-West Atlantic region, *Earth Planet. Sci. Lett.*, 2005, vol. 236, pp. 249–257. doi 10.1016/j.epsl.2005.05.029
- Laske, G., Masters, G., Ma, Z., and Pasyanos, M., *Update on CRUST1.0—A 1-degree global model of Earth's crust*, *Geophys. Res. Abstr.*, 2013, vol. 15, Abstr. EGU 2013-2658.
- Lebedeva-Ivanova, N.N., Zamansky, Y.Ya., and Länginen, A.E., Seismic profiling across the Mendeleev Ridge at 82° N: evidence of continental crust, *Geophys. J. Int.*, 2006, vol. 165, pp. 527–544. doi 10.1111/j.1365-246X.2006.02859.x
- Levshin, A.L., Yanovskaya, T.B., Lander, A.V., Bukchin, B.G., Barmin, M.P., Ratnikova L.I., and Its, Ye.N., *Poverkhnostnye seismicheskie volny v gorizontally'no-neodnorodnoi Zemle* (Surface Seismic Waves in a Horizontally Inhomogeneous Earth), Moscow: Nauka, 1986.
- Levshin, A.L., Ritzwoller, M.H., Barmin, M.P., Villaseñor, A., and Padgett, C.A., New constraints on the arctic crust and uppermost mantle: surface wave group velocities, Pn, and Sn, *Phys. Earth Planet. Inter.*, 2001, vol. 123, nos. 2–4, pp. 185–204.
- Levshin, A.L., Schweitzer, J., Weidle, C., Shapiro, N.M., and Ritzwoller, M.H., Surface wave tomography of the Barents Sea and surrounding regions, *Geophys. J. Int.*, 2007, vol. 170, pp. 441–459. doi 10.1111/j.1365-246X.2006.03285.x
- Olsson, S., Roberts, R.G., and Bödvarsson, R., Analysis of waves converted from S to P in the upper mantle beneath the Baltic Shield, *Earth Planet. Sci. Lett.*, 2007, vol. 257, nos. 1–2, pp. 37–46.
- Pedersen, H.A., Debayle, E., Maupin, V., and the POLENET/LAPNET Collab., Strong lateral variations of lithospheric mantle beneath cratons—example from the Baltic shield, *Earth Planet. Sci. Lett.*, 2013, vol. 383, pp. 164–172. <http://dx.doi.org/10.1016/j.epsl.2013.09.024>
- Pilidou, S., Priestley, K., Gudmundsson, O., and Debayle, E., Upper mantle S-wave speed heterogeneity beneath the North Atlantic from regional surface wave tomography: the Iceland and Azores plumes, *Geophys. J. Int.*, 2004, vol. 159, pp. 1057–1076. doi 10.1111/j.1365-246X.2004.02462.x
- Pilidou, S., Priestley, K., Debayle, E., and Gudmundsson, O., Rayleigh wave tomography in the North Atlantic: high resolution images of the Iceland, Azores and Eifel mantle plumes, *Lithos*, 2005, vol. 79, pp. 453–474. doi 10.1016/j.lithos.2004.09.012
- Rickers, F., Fichter, A., and Trampert, J., The Iceland-Jan Mayen plume system and its impact on mantle dynamics in the North Atlantic region: evidence from full-waveform inversion, *Earth Planet. Sci. Lett.*, 2013, vol. 367, pp. 39–51. <http://dx.doi.org/10.1016/j.epsl.2013.02.022>
- Ritzwoller, M.H. and Levshin, A.L., Eurasian surface wave tomography: group velocities, *J. Geophys. Res.*, 1998, vol. 103, pp. 4839–4878.

- Schaeffer, A.J. and Lebedev, S., Global shear speed structure of the upper mantle and transition zone, *Geophys. J. Int.*, 2013, vol. 194, pp. 417–449. doi 10.1093/gji/ggt095
- Schilling, J.G., Kingsley, R., Fontignie, D., Poreda, R., and Xue, S., Dispersion of the Jan Mayen and Iceland mantle plumes in the Arctic: a He–Pb–Nd–Sr isotope tracer study of basalts from the Kolbeinsey, Mohns and Knipovich Ridges, *J. Geophys. Res.*, 1999, vol. 10, no. 5, pp. 10543–10569.
- Shapiro, N.M. and Ritzwoller, M.H., Monte-Carlo inversion for a global shear-velocity model of the crust and upper mantle, *Geophys. J. Int.*, 2002, vol. 151, pp. 88–105.
- Verhoef, J., Roest, W.R., Macnab, R., Arkani-Hamed, J. and Project Team, *Magnetic Anomalies of the Arctic and North Atlantic Oceans and Adjacent Land Areas*. Geological Survey of Canada, Open File Report 3125a, 1996
- Yanovskaya, T.B., *Development of the methods for solving the problems of surface-wave tomography based on the Backus–Gilbert method*, *Vychislit. Seismol.*, vol. 32, Moscow: GEOS, 2001, pp. 11–26
- Yanovskaya, T.B. *Poverkhnostno-volnovaya tomografiya v seysmologicheskikh issledovaniyakh* (Surface Wave Tomography in Seismological Studies), St.-Petersburg: Nauka, 2015.
- Yanovskaya, T.B. and Kozhevnikov, V.M., 3D S-wave velocity pattern in the upper mantle beneath the continent of Asia from Rayleigh wave data, *Phys. Earth Planet. Inter.*, 2003, vol. 138, pp. 263–278.
- Yanovskaya, T.B., Antonova, L.M., Kozhevnikov, V.M., Lateral variations of the upper mantle structure in Eurasia from group velocities of surface waves, *Phys. Earth Planet. Inter.*, 2000, vol. 122, pp. 19–32.
- Zhou, Y., Nolet, G., Dahlen, F.A., and Laske, G., Global upper-mantle structure from finite-frequency surface-wave tomography, *J. Geophys. Res.*, 2006, vol. 111, B04304. doi 10.1029/2005JB003677
- Zonenshain, L.P. and Natapov, L.M., Tectonic history of the Arctic, in *Aktual'nye problemy tektoniki* (Current Issues in Tectonics), Moscow: Nauka, 1987, pp. 31–57.
- Zonenshain, L.P., Kuzmin, M.I., and Natapov, L.M., *Tektonika litosfernykh plit territorii SSSR* (Tectonics of Lithospheric Plates in the USSR Territory), Moscow: Nedra, 1990, Book 2.

Translated by M. Nazarenko